Roads to the Standard Model

Rodrigo Alonso and Mia West

Institute for Particle Physics Phenomenology, Durham University, South Road, Durham, DH1 3LE, United Kingdom

(Received 26 October 2021; accepted 12 April 2022; published 25 May 2022)

Experimental measurements point at the Standard Model (SM) as the theory of electroweak symmetry breaking, but as we close in on our characterization the question arises of what limits in theory space lead to the SM. The class of theories with this property cannot be ruled out, only constrained to an ever smaller neighborhood of the SM. In contrast, which class of theories does not possess this limit and can therefore potentially be ruled out experimentally? In this work we study both classes and find evidence to support the Standard Model effective field theory being the single road to the Standard Model, theories that fall outside this class keeping a "minimum distance" from the SM characterized by a cutoff of at most $4\pi v/g_{\mathrm{SM}}$.

DOI: 10.1103/PhysRevD.105.096028

I. INTRODUCTION

Nowadays, particle physics finds itself in the midst of electroweak symmetry breaking (EWSB) exploration, and the outcome of this endeavor will chart nature's theory of elementary particles. Experimental data collated and compared with predictions of theories of EWSB have narrowed down the range possibilities; many casualties lie indeed now discarded having been disproven by the progress in our measurements. The Higgs boson discovery, coming up on a decade old, was the main stroke in our map, subsequent data giving a profile that resembles the one heralded by the Standard Model (SM). Theory considerations have long pointed out the SM case for EWSB to be unstable under higher scale corrections and indicated that new physics should lie in wait at the electroweak scale. Whether these considerations should be revisited and our theory perspective profoundly changed, or if instead patience is all that is needed, the pressing question at present posed by experimental data is to characterize the theory "neighborhood" of the SM. The claim that one observes nothing but the SM at the LHC is indeed only as good as our characterization of what else we could observe; it is here we find value in the aforementioned casualties. The aim in this work is to explore the consistent theory neighborhood of the Standard Model.

A long known and studied approach, or "trajectory," to the SM is a linearly realized effective field theory (SMEFT) (see [1] for a review), this road being pointed at by the decoupling theorem [2]. The integration of any heavy particle whose mass can be arbitrarily larger than the EWSB vacuum expectation value (VEV) ($M > v$) in a perturbative linear realization will yield the SMEFT; supersymmetry or composite Higgs models fall into this category. Is this the only road to the Standard Model; i.e., are there other consistent limits to obtain the SM couplings for the known spectrum of elementary particles? As fundamental as this topic is, on its present formulation the candidate preceded the question; Higgs effective theory (HEFT) [3,4] is an EFT that encompasses the SMEFT but extends beyond it and might offer new roads. In HEFT, a linear realization is not assumed (though admissible in a certain limit) and is indeed the most general Lorentz and gauge invariant theory with the known spectrum of particles (which suggests it should be possible to formulate it in terms of amplitudes). The theories that this EFT describes but fall out of SMEFT, which will be called here theories of the quotient space HEFT/SMEFT or simply quotient EFTs,[1] could contain a path to the SM other than via SMEFT. This quotient space is characterized as missing a point in field space which is left invariant under an $O(4)$ transformation [5,6], be it because it is not present or because the would-be invariant point is singular [7]. A geometric formalism was used to derive this result and also aids in exploring the properties of theories without field redundancies, as introduced in [5,6], and followed up in [7–9]—it is also adopted here. Some theories in HEFT/SMEFT quotient space have been formulated while having a perturbative expansion [7]; they have been found to have a cutoff of $\sim 4\pi v$, and no limit can be taken within them that yields the SM. It has been suggested that *all* of this quotient space shares this property of a finite v-bound cutoff [10]

[1] In other works these are called, with a slight abuse of notation, HEFT.

with further evidence provided in [9], which means in turn that they all could be casualties of our exploration with present and future machines. This question has been explored so far with perturbative unitarity bounds, while here it is looked at with semiclassical arguments.

This article is structured as follows. Section II introduces geometry from amplitudes, and Sec. II A presents the basis in Riemann normal coordinates. This first part has been rendered review, rather than new results, by virtue of [9] although all results here are derived independently. Section II B presents theory and experimental bounds on the curvature plane while Sec. III characterizes SMEFT on this plane. In Sec. IV, example models of SMEFT and quotient space are presented and characterized in the curvature plane. Section V presents theories in quotient space arising from geometry rather than explicit models and finds candidate quotient theories that seem to approach the SM. A semiclassical argument for the finite cutoff of theories in quotient space is given in Sec. VI.

II. GEOMETRY AND AMPLITUDES

For simplicity, $O(4) \supset SU(2) \times U(1)$ invariance in the EWSB sector is assumed. We take the high energy limit and make use of the equivalence theorem. These approximations allow us to focus on a subset of possible modifications of the bosonic sector. The Higgs singlet field is denoted h, and the Goldstones swallowed by the W and Z bosons as φ^a, $a = 1, 2, 3$.

Let us start by defining our geometry from the scattering-matrix S in order to depart from a common-place, basis-invariant magnitude in particle physics. Following the line-integral definition for general amplitudes valid also in the UV, we have ($S = 1 - i\mathcal{A}$)

$$-R_{h+h-} = \frac{1}{2\pi i}\oint \frac{1}{s_{12}^2}\mathcal{A}_{W_1^+W_2^-\to hh}, \tag{1}$$

$$-R_{+-+-} = \frac{1}{2\pi i}\oint \frac{1}{s_{12}^2}\mathcal{A}_{W_1^+W_2^+\to W^+W^+}, \tag{2}$$

$$-\nabla_h R_{+h-h} = \frac{1}{2\pi i}\oint \frac{1}{s_{12}^2}\mathcal{A}_{W_1^+W_2^-\to hhh}, \tag{3}$$

$$-\nabla_h R_{+-+-} = \frac{1}{\pi i}\oint \frac{1}{s_{12}^2}\mathcal{A}_{W_1^+W_2^+\to W_3^+W_4^+h}, \tag{4}$$

$$= \frac{1}{\pi i}\oint \frac{1}{s_{34}^2}\mathcal{A}_{W_1^+W_2^+\to W_3^+W_4^+h}, \tag{5}$$

where $s_{ij} = (p_i + p_j)^2$. Indices in the Riemann tensor run through h, $a = 1, 2, 3$, and the $\pm$ entries are given by contracting an a index with the projector $(\delta_1^a \pm i\delta_2^a)/\sqrt{2}$, for example,

$$R_{h+h-} = R_{hahb}\frac{(\delta_1^a + i\delta_2^a)}{\sqrt{2}}\frac{(\delta_1^b - i\delta_2^b)}{\sqrt{2}}. \tag{6}$$

While the above definition is useful to include UV models and derive positivity bounds [11], in practice we will work with the low energy EFT. In this case the correspondence is taking our geometry from the order $\mathcal{O}(s)$ coefficients in a Taylor expansion. What is more, they capture all terms to this order. Being explicit,

$$\mathcal{A}_{W_1^+W_2^-\to hh} = -s_{12}R_{+h-h}, \tag{7}$$

$$\mathcal{A}_{W_1^+W_2^+\to WW} = -s_{12}R_{+-+-}, \tag{8}$$

$$\mathcal{A}_{W_1^+W_2^-\to hhh} = -s_{12}\nabla_h R_{+h-h}, \tag{9}$$

$$\mathcal{A}_{W_1^+W_2^+\to W_3^+W_4^+h} = -\frac{s_{12}+s_{34}}{2}\nabla_h R_{+-+-}, \tag{10}$$

where we neglected masses assuming $s \gg M_W^2, M_Z^2, m_h^2$.

This starting point makes it evident that our tensor, R, and its derivatives are physical and field redefinition (coordinate) invariant. Even if intuitive, this last statement should be qualified. On the geometry side, having defined tensor entries rather than invariants, one has that these change under coordinate transformations—albeit with well-defined properties. They are nonetheless the same for local (defined around the vacuum) transformations of our fields which leave the amplitudes the same [12]:

$$\hat{\phi}^i = \left(\delta_j^i + \sum_{k=1} c_j^k \phi^k\right)\phi^j, \tag{11}$$

so that after quantization both fields produce a particle out of the vacuum,

$$\langle p|\phi^i|0\rangle = \langle p|\hat{\phi}^i|0\rangle \tag{12}$$

with $|p\rangle$ the state associated with the field. It is for this type of transformation that the S matrix will be left invariant, and tensors evaluated at the vacuum transform trivially, since

$$\left.\frac{\partial\phi^i}{\partial\hat{\phi}^j}\right|_{\phi=0} = \delta_j^i. \tag{13}$$

Still, from where we stand the definition of Riemann tensor components in terms of amplitudes seems arbitrary and potentially inconsistent. So let us now turn to the Lagrangian theory which yields such relations.

A. Riemann normal coordinates

Take the metric from which the Riemann tensor derives in Eqs. (1)–(5) as $G_{ij}(\phi)$, with $i, j = h, 1, 2, 3$, $\phi = (h, \varphi^a)$,

$a = 1, 2, 3$. The amplitudes in Eqs. (1)–(5) follow from the action

$$S = \frac{1}{2}\int d^4x \partial_\mu \phi^i G_{ij} \partial^\mu \phi^i$$
$$= \frac{1}{2}\int d^4x (\partial_\mu h \partial^\mu h + F(h)^2 g_{ab} \partial^\mu \varphi^a \partial_\mu \varphi^b). \quad (14)$$

In matrix notation, our parametrization of the metric reads

$$G_{ij} = \begin{pmatrix} 1 & \\ & F^2 g_{ab} \end{pmatrix}, \quad (15)$$

where off-diagonal entries are forbidden by symmetry and g_{ab} is the metric on the three-sphere, which we find useful to represent via the unit vector $u(\varphi)$:

$$g_{ab} = \frac{\partial u(\varphi)}{\partial \varphi^a} \frac{\partial u(\varphi)}{\partial \varphi^b}, \qquad u \cdot u = 1, \quad (16)$$

with u transforming as a vector under $O(4)$. It follows that the nonvanishing elements of the Riemann tensor and its first covariant derivative are

$$R_{abcd} = \left(\frac{1}{v^2} - (F')^2\right) F^2 g_{a[c} g_{bd]}, \quad (17)$$

$$R_{ahbh} = -F'' F \tilde{g}_{ab}, \quad (18)$$

$$\nabla_h R_{ahbh} = F^2 \left(-\frac{F''}{F}\right)' g_{ab}, \quad (19)$$

$$\nabla_h R_{abcd} = F^4 \left(\frac{1}{v^2 F^2} - \frac{(F')^2}{F^2}\right)' g_{a[c} g_{bd]}, \quad (20)$$

$$\nabla_a R_{hbcd} = \frac{F^4}{2} \left(\frac{1}{v^2 F^2} - \frac{(F')^2}{F^2}\right)' g_{a[c} g_{bd]}, \quad (21)$$

where the prime denotes differentiation with respect to h and it is useful to define

$$R_h \equiv -\frac{F''}{F}, \qquad R_\varphi \equiv \frac{1}{v^2 F^2} - \frac{(F')^2}{F^2}. \quad (22)$$

Verifying that these tensor entries appear as coefficients in the four- and five-point amplitudes is a matter of computing amplitudes: expanding our metric around the vacuum and adding over the various diagrams (e.g., see Fig. 1 for those contributing to $WW \to hhh$), relations (1)–(5) are recovered. The $O(4)$ symmetry in our system reduces the number of independent components and amplitudes to R_h, R_φ, and its derivatives.

Geometry does tell us, however, that there is a frame where this computation is particularly simple: the frame where our coordinates follow geodesics, i.e., Riemann normal coordinates (RNC).

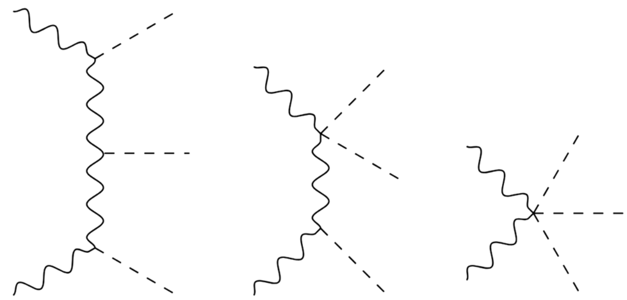

FIG. 1. Diagrams for the $\mathcal{O}(s)$ contribution to the $WWhhh$ amplitude in the basis of Eq. (14).

Let us then go into a brief outline of RNC. One can solve iteratively the geodesic equation

$$\frac{d^2\phi^i}{d\sigma^2} + \Gamma^i_{jk}(\phi) \frac{d\phi^j}{d\sigma} \frac{d\phi^k}{d\sigma} = 0 \quad (23)$$

in an expansion that assumes the dependence on ϕ of Γ, admits a Taylor expansion, and introduces new coordinates ϕ' defined to second order as

$$\phi'^i = \phi^i + \frac{1}{2}\Gamma^i_{jk}(0)\phi^j\phi^k + \mathcal{O}(\phi^3).$$

Together with a metric in the new coordinates and to ϕ'^3 order [13]

$$G(\phi')_{ij} = G(0)_{ij} + \phi'^k \phi'^l \frac{1}{3} R_{iklj} + \frac{1}{6}\phi'^k \phi'^l \phi'^m \nabla_m R_{iklj}.$$

For concreteness, one can work out this transformation for our metric to find

$$\begin{pmatrix} h' \\ \varphi' \end{pmatrix} = \begin{pmatrix} h - FF'\varphi^2/2 \\ \varphi^a + F'h\varphi^a/F + \Gamma^a_{bc}\varphi^b\varphi^c/2 \end{pmatrix} + \mathcal{O}(\phi^3).$$

The use of RNC is the reduction to parametrization independent magnitudes, i.e., the Riemann tensor and its derivatives with the Christoffel symbols absent in our frame. In an analogy with general relativity, this is the free-falling frame where tidal effects reveal the geometry of the spacetime manifold. In practice, there are no three-point amplitudes[2] and the interacting Lagrangian for four-point reads

[2]They are reinstated, however, once we account for massive states.

$$\mathcal{L}_4^{\mathrm{RNC}} = \frac{1}{6} R_{hahb}(2h\partial h\varphi^a \partial\varphi^b - (\partial h)^2\varphi^a\varphi^b - h^2\partial\varphi^a\partial\varphi^b) + \frac{1}{6} R_{abcd}\partial\varphi^a\varphi^b\varphi^c\partial\varphi^d. \tag{24}$$

The first line gives the Feynman rule

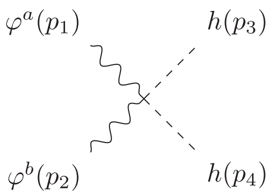

$$\frac{iR_{ahbh}}{3}\begin{pmatrix} (p_1+p_2)(p_3+p_4) \\ +2p_1p_2+2p_3p_4 \end{pmatrix}$$

which evaluated on-shell is the sole diagram needed to compute $A_{WW\to hh}$ in this frame. For five-point vertexes, we have

$$\mathcal{L}_5^{\mathrm{RNC}} = \frac{1}{12}(\nabla_h R_{\partial\varphi hh\partial\varphi} + \nabla_h R_{\partial h\varphi\varphi\partial h} + 2\nabla_h R_{\partial h\varphi h\partial\varphi}) + \frac{1}{12}(\nabla_h R_{\partial\varphi\varphi\varphi\partial\varphi} + 2\nabla_\varphi R_{\partial\varphi h\varphi\partial\varphi}) \tag{25}$$

where the term $\nabla_\varphi R_{dh\varphi\varphi d\varphi}$ cancels due to the Riemann tensor asymmetry; and with abuse of notation $V_\varphi = V_a\varphi^a$, similarly for h. For the 5-point amplitude, again due to the absence of 3-point vertices, evaluating the Feynman rule that follows from the five-point action yields the result (i.e., in this frame there is only the last diagram in Fig. 1 to compute). Amplitudes for six or more particles in total do require a sum over diagrams and contain, in addition, poles that nevertheless can be derived from lower-point amplitudes (see [9]).

A general EFT also has modifications in the pure gauge and fermionic sectors as, e.g., a metric for the gauge kinetic terms [8,14]; these are subleading in the high energy limit and for the observables here considered, although in practice they should be included in a complete analysis, which we leave for future work.

B. Experimental and theory constraints on curvature

Unitarity constrains the magnitude of curvature, and its derivatives, for a given centre of mass energy s, to the four-point level. Symbolically

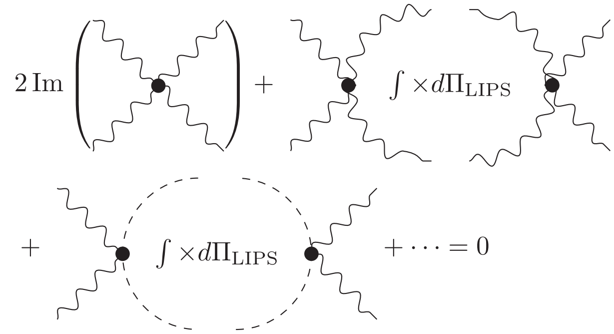

where the first partial wave for W^+W^- gives

$$\left(\frac{R_\varphi s}{16\pi}\right)^2 + \frac{1}{2}\left(\frac{R_h s}{8\pi}\right)^2 \leq 1, \tag{26}$$

where we have accounted for the amplitude being real. One can also select the W^+W^+ channel, but the emphasis in here is on bounds that are sensitive to both curvatures simultaneously, which helps to better close some corners in the curvature plane.

One can use these constraints to determine the theory cutoff in terms of curvature; however, here we turn this around to note that given that we have explored energies up to $s \sim v^2$ and no new states have showed up, we can set an upper limit on curvature.

This limit is superseded by experimental bounds from LHC which bound Higgs couplings. In the conventional parametrization, one has

$$F(h)^2 = 1 + 2a\frac{h}{v} + b\frac{h^2}{v^2} + \mathcal{O}(h^3), \tag{27}$$

which gives a curvature around the origin

$$v^2(R_\varphi(0), R_h(0)) = (1-a^2, -(b-a^2)), \tag{28}$$

itself related to amplitudes as, substituting (22), (17), (18) in (7) and (8),

$$\mathcal{A}_{W_1^+W_2^+\to WW} = s_{12}R_\varphi, \tag{29}$$

$$\mathcal{A}_{W_1^+W_2^-\to hh} = -s_{12}R_h. \tag{30}$$

Translating bounds on the coefficients from present and future measurements into curvature,[3] we present the plot in Fig. 2. The value in both sets of constraints is to put into context how much of the theory-consistent curvature space have we explored experimentally.

[3]Implicit in the relation of curvature and amplitudes is the assumption of no pure gauge sector modification justifiable given stringent constraints from LEP.

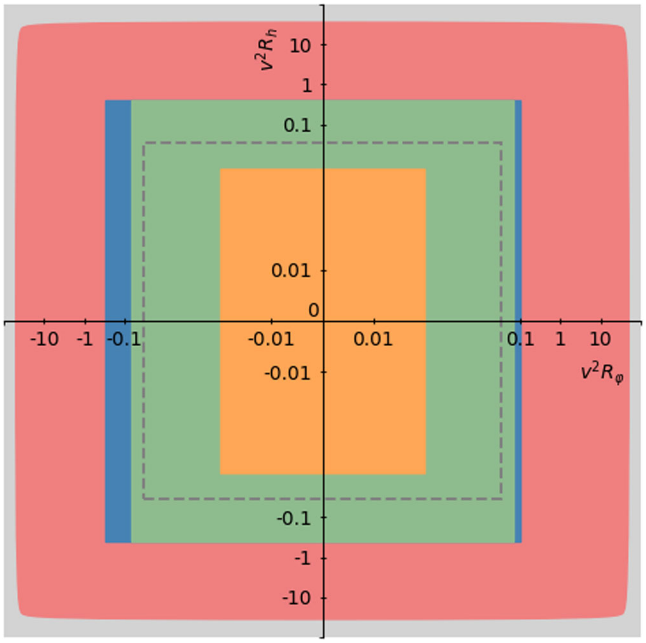

FIG. 2. Theoretically (gray) and experimentally (up to blue) excluded (up to 95% confidence level) regions of the curvatures R_h, R_φ which are related to electroweak amplitudes as in Eqs. (30) and (29); and sensitivity limits of future colliders (HL-LHC, up to green; FCC, up to orange), also up to 95% confidence level. See text for details. The plot scales linearly within the dashed box and logarithmically outside.

From the outermost to the innermost region of Fig. 2: the (outermost) gray region is excluded due to unitarity; up to the blue region is excluded by current LHC bounds (the region is translated from bounds on a in [15], and b in [16]); finally, up to the green and orange (innermost) regions we present expected exclusion limits for HL-LHC and FCC, respectively. The projected bounds on R_φ, R_h are derived using sensitivity predictions of a (HL-LHC [17]; FCC-ee [18]), and b ([19] for both HL-LHC and FCC-hh), around their SM values. All uncertainties and projected sensitivities are displayed at the 95% confidence level, where multiple sensitivity estimates are given, and the most conservative is selected. Note that HL-LHC bounds used here predate the LHC ones so that the seemingly marginal improvement is likely an underestimation.

III. CORRELATION OF CURVATURE IN SMEFT

In the linear realization and to first order [with our assumption of $O(4)$ invariance] we have

$$R_\varphi = R_h, \tag{31}$$

which is to say the coefficients of s in the four-point amplitudes for W^+W^+ scattering and $W^+W^- \to hh$ in Eqs. (30) and (29) are anticorrelated. Correlations do appear in the linear parametrization of SMEFT in HEFT [20] in line with what we find here; nonetheless, in this section we go into some length of how this can be derived to display the utility of a geometric language.

A simple argument to show there is a correlation, if a bit more abstract, is to use Riemann normal coordinates and custodial symmetry around the $O(4)$-symmetric point—which admits Cartesian coordinates. In this frame, the metric reads

$$G_{ij}(\phi) = \delta_{ij} + \frac{1}{3} R_{iklj} \phi^k \phi^l + \mathcal{O}(\phi^3), \tag{32}$$

and a linear realization of $O(4)$ symmetry dictates that the Riemann tensor be of the form $R(\delta_{il}\delta_{kj} - \delta_{kl}\delta_{ij})$, with a single unknown R. A transformation from Cartesian to polar coordinates then reveals $R_h = R_\varphi$.

The collapse of the two curvatures into a single one can also be derived matching the two EFTs:

$$\frac{(\partial h^2 + F^2 \partial\varphi^2)}{2} = K\left(\frac{H^\dagger H}{M^2}\right)(\partial H^\dagger H)^2 + G\left(\frac{H^\dagger H}{M^2}\right) D_\mu H^\dagger D^\mu H, \tag{33}$$

where it should be understood from a general SMEFT action; we transformed to a basis where the Higgs singlet is canonically normalized.

This exercise yields to order M^{-4}

$$R_\varphi = -3\frac{G'(0)}{M^2} + \frac{H^\dagger H}{M^4}\left(2(G'(0))^2 - \frac{5}{2} G''(0)\right), \tag{34}$$

$$R_h = -3\frac{G'(0)}{M^2} + \frac{H^\dagger H}{M^4}(4(G'(0))^2 - 5G''(0)), \tag{35}$$

which also reveals the correlation is lost at order M^{-4}.

Finally, and in a direct connection with observables, one can compute the amplitude that has been used to define our curvature, the computation itself getting rid of any field redundancy. Take the noncanonically normalized action

$$\mathcal{L} = \frac{1}{2}\frac{c_{H\Box}}{M^2}(\partial_\mu H^\dagger H)^2 + \frac{c_{HDD}}{M^2} H^\dagger H D_\mu H^\dagger D^\mu H. \tag{36}$$

After normalization of the theory, the computation of diagrams such as those shown in Fig. 3, where we note that in this frame there is a h^3 coupling that scales with s and must be accounted for, yields

$$\mathcal{A}_{W^+W^+\to W^+W^+} = \frac{s}{M^2}(c_{H\Box} - c_{HDD}), \tag{37}$$

$$\mathcal{A}_{W^+W^-\to hh} = -\frac{s}{M^2}(c_{H\Box} - c_{HDD}), \tag{38}$$

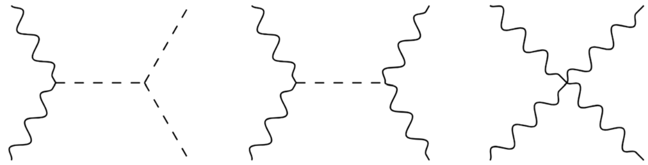

FIG. 3. A selection of diagrams for the $WWhh$ and $WWWW$ amplitudes with the action in Eq. (36).

and hence the direct connection with SMEFT geometry as

$$(R_\varphi, R_h) = \frac{1}{M^2}(c_{H\Box} - c_{HDD}, c_{H\Box} - c_{HDD}). \quad (39)$$

IV. MODELS AS PROBES INTO HEFT

Recent study of EFT has shown that UV completion might impose extra constraints on an otherwise seemingly valid EFT, as is the case of positivity constraints [21]. It should be said that these constraints on the curvatures themselves R_h and R_φ do not restrict their sign but reveal the need for doubly charged states if the curvature is negative [11]. It is for these reasons that this section looks at models and introduces two new representations under $O(4)$ as

$$\mathbf{h}\colon\ 4 \text{ of } O(4), \quad (40)$$

$$\Phi\colon\ 9 \text{ of } O(4) \text{ (traceless symmetric)}, \quad (41)$$

$$S\colon\ 1 \text{ of } O(4), \quad (42)$$

with the results of positivity constraints suggesting S and Φ will produce positive and negative curvatures, respectively. Note that $\mathbf{h}$ is the Higgs doublet H in a real representation as

$$(\tilde{H}, H) = \hat{\sigma}_I \frac{\mathbf{h}^I}{\sqrt{2}} \quad (43)$$

with $\tilde{H} = \epsilon H^*$ and $\sigma^I = (\sigma^i, 1)$ with σ^i the Pauli matrices. We consider the addition of a 9 and a 1 separately with respective actions

$$\mathcal{L}_S = \frac{1}{2} D_\mu \mathbf{h}^T D_\mu \mathbf{h} + \frac{1}{2}(\partial S)^2 - V(\mathbf{h}, S^2), \quad (44)$$

$$\mathcal{L}_\Phi = \frac{1}{2} D_\mu \mathbf{h}^T D_\mu \mathbf{h} + \frac{1}{2}\mathrm{Tr}(D_\mu \Phi D^\mu \Phi) - V(\mathbf{h}, \Phi). \quad (45)$$

The key distinction is whether $\langle\Phi\rangle = 0$, which depends on the sign of its mass term and its mixing as induced by the potential.

A. Only h acquires a VEV, SMEFT case

In this subsection we momentarily restrict the $O(4)$ symmetry to $SO(4)$ to allow for trilinear couplings. First, for the singlet S case, we take a potential as

$$V = -\frac{g_* m_S}{2} S\mathbf{h}^2 + \frac{m_S^2}{2} S^2 + \frac{m_{\mathbf{h}}^2}{2}\mathbf{h}^2; \quad (46)$$

extra terms allowed by the symmetry will give controlled corrections to the result, and we neglect them. Integrating the field S at tree level returns

$$\mathcal{L}_{\mathrm{eff}} = \frac{1}{2}\frac{g_* m_S}{2}\mathbf{h}^2 \frac{1}{\partial^2 + m_S^2}\frac{g_* m_S}{2}\mathbf{h}^2 \quad (47)$$

$$= \frac{g_*^2}{2}(H^\dagger H)^2 + \frac{g_*^2}{2m_S^2}(\partial(H^\dagger H))^2 + \mathcal{O}(\partial^4), \quad (48)$$

and then via Eq. (39)

$$(R_\varphi, R_h) = \left(\frac{g_*^2}{m_S^2}, \frac{g_*^2}{m_S^2}\right), \quad (49)$$

i.e., positive curvature for the singlet case, as expected.

Along the same lines, the potential for the symmetric representation is

$$V = -\frac{g_* m_\Phi}{2}\mathbf{h}^T\Phi\mathbf{h} + \frac{m_\Phi^2}{2}\Phi^2 + \frac{m_{\mathbf{h}}^2}{2}\mathbf{h}^2. \quad (50)$$

The integration now returns to dimension six:

$$\begin{aligned}\mathcal{L}_{\mathrm{eff}} &= \frac{g_*^2}{8}\mathrm{Tr}\left[\left(\mathbf{h}\mathbf{h}^T - \frac{\mathbf{h}^2}{4}\right)\frac{m_\Phi^2}{\Box + m_\Phi^2}\left(\mathbf{h}\mathbf{h}^T - \frac{\mathbf{h}^2}{4}\right)\right] \\ &= \frac{3g_*^2}{8}(H^\dagger H)^2 + \frac{g_*^2}{m_\Phi^2}\left(H^\dagger H D H^\dagger D H + \frac{(\partial H^\dagger H)^2}{8}\right),\end{aligned} \quad (51)$$

where $\Box = D_\mu D^\mu$ and one has that the operator does yield negative curvature:

$$(R_\varphi, R_h) = \left(-\frac{3g_*^2}{4m_\Phi^2}, -\frac{3g_*^2}{4m_\Phi^2}\right). \quad (52)$$

B. Both Φ and h break the symmetry, HEFT/SMEFT quotient space

As we will show, this case does not belong in SMEFT and stands as a representative of quotient space. We take the extension of a mexican hat potential for two fields as

$$V(\Phi) = -\frac{\vec{m}^2}{2}\cdot\begin{pmatrix}\mathbf{h}^2\\ \Phi^2\end{pmatrix} + \begin{pmatrix}\mathbf{h}^2\\ \Phi^2\end{pmatrix}^T \frac{\lambda}{8}\begin{pmatrix}\mathbf{h}^2\\ \Phi^2\end{pmatrix} - \frac{\tilde{\lambda}}{8}\mathbf{h}^T\Phi\Phi\mathbf{h} + \frac{\tilde{\lambda}_\Phi}{8}\mathrm{Tr}(\Phi\Phi\Phi\Phi) \tag{53}$$

with $\vec{m}^2$ a two-vector and λ a 2×2 symmetric matrix. Since Φ acquires a VEV, we take $\tilde{\lambda} > 0$, which triggers $O(4) \to O(3)$ and preserves custodial symmetry. Linear terms in the fields are absent, contrary to the previous case where we restore $O(4)$ in place of $SO(4)$. The key question as will be shown is to consistently compute particle couplings and masses from an explicit potential.

The Goldstone boson Lagrangian and couplings to the radial singlet modes δh, $\delta\Phi$ read

$$\mathcal{L} = \frac{1}{2}((v_{\mathbf{h}} + \delta h)^2 + C_9(v_\Phi + \delta\Phi)^2)\frac{g_{ab}}{v^2}D^\mu\varphi^a D_\mu\varphi^b, \tag{54}$$

where

$$C_9 = \frac{2\times 4}{4-1}, \qquad v^2 = v_{\mathbf{h}}^2 + C_9 v_\Phi^2, \qquad \sin\beta = \sqrt{C_9}\frac{v_\Phi}{v}, \tag{55}$$

and

$$\langle\mathbf{h}\rangle = \begin{pmatrix}0\\0\\0\\v_{\mathbf{h}}\end{pmatrix}, \quad \langle\Phi\rangle = \frac{v_\Phi}{2\sqrt{3}}\begin{pmatrix}1&&&\\&1&&\\&&1&\\&&&-3\end{pmatrix}, \tag{56}$$

the generalization of C_9 to $SO(N)$ being $C_{N(N+1)/2-1} = 2N/(N-1)$. Take the mixing for the singlet radial modes $\delta\mathbf{h}$ and $\delta\Phi$ as [note that no other field in Φ or $\mathbf{h}$ is a singlet of $SO(3)$ so we know these two only mix among each other]:

$$\begin{pmatrix}\delta\mathbf{h}\\ \delta\Phi\end{pmatrix} = \begin{pmatrix}\cos\omega & -\sin\omega\\ \sin\omega & \cos\omega\end{pmatrix}\begin{pmatrix}h\\ \tilde{h}\end{pmatrix}. \tag{57}$$

Putting the above back in the Lagrangian for the Goldstones and taking h to be the lightest singlet, one obtains in our basis of Eqs. (14) and (27)

$$a = c_\omega c_\beta + \sqrt{C_9}s_\beta s_\omega, \qquad b = c_\omega^2 + C_9 s_\omega^2. \tag{58}$$

Note that the limit of no mixing gives $b = 1$ and a parametrization of the curvature $R_h = -R_\varphi$ orthogonal to the SMEFT with a potential new road to the SM. The question to be answered is then: can one take $\omega = \beta = 0$ while keeping $m_{\tilde{h}} \gg m_h$ and maintaining perturbativity?

To answer this question we should express ω and β in terms of physical masses and couplings, and then use Eq. (28) to substitute and find curvature as a function of physical masses and couplings. In practice we have to solve for the potential. The value of the fields that minimize V can be read off after rearranging as

$$V(v_{\mathbf{h}}, v_\Phi) = (\vec{v}^2 - 2\hat{\lambda}^{-1}\vec{m}^2)^T\frac{\hat{\lambda}}{8}(\vec{v}^2 - 2\hat{\lambda}^{-1}\vec{m}^2) \tag{59}$$

with

$$\vec{v}^2 = 2\hat{\lambda}^{-1}\vec{m}^2, \qquad \hat{\lambda} = \lambda + \begin{pmatrix} & -3\tilde{\lambda}/8\\ -3\tilde{\lambda}/8 & 7\tilde{\lambda}_\Phi/12\end{pmatrix}. \tag{60}$$

Next, expanding around the VEVs we find the mass matrix for the singlets $\delta\mathbf{h}, \delta\Phi$ as

$$M^2 = \mathrm{Diag}(v)\hat{\lambda}\,\mathrm{Diag}(v) = U\,\mathrm{Diag}(m_h^2, m_{\tilde{h}}^2)U^T \tag{61}$$

with $\mathrm{Diag}(v) = \delta^{ij}v_j$. The aim is to express ω, β as $\omega(m_h, m_{\tilde{h}}, \hat{\lambda}, v), \beta(m_h, m_{\tilde{h}}, \hat{\lambda}, v)$, which can be done by taking the determinant of the mass matrix

$$\det(M^2) = v_{\mathbf{h}}^2 v_\Phi^2 \det(\hat{\lambda}) = m_h^2 m_{\tilde{h}}^2 \tag{62}$$

and combining the eigenvector equations into

$$\sin(2\omega) = \frac{2v_{\mathbf{h}}v_\Phi}{m_h^2 - m_{\tilde{h}}^2}\hat{\lambda}_{\mathbf{h}\Phi} \tag{63}$$

to obtain

$$\sin(2\omega) = \frac{2m_h m_{\tilde{h}}}{m_h^2 - m_{\tilde{h}}^2}\frac{\hat{\lambda}_{\mathbf{h}\Phi}}{\sqrt{\det(\hat{\lambda})}}, \tag{64}$$

$$\sin(2\beta) = \sqrt{C_9}\frac{2m_h m_{\tilde{h}}}{v^2\sqrt{\det\hat{\lambda}}}. \tag{65}$$

No obstacle prevents taking $\omega \to 0$ with $\hat{\lambda}_{\mathbf{h}\Phi} \to 0$, but it is evident that β cannot be arbitrarily close to zero while keeping $\tilde{h}$ massive and respecting unitarity. Qualitatively then, we have a minimum attainable curvature as

$$\left(v^2 R_\varphi \geq \frac{3m_h^2 m_{\tilde{h}}^2}{8\pi^2 v^4}, v^2 R_h \leq -\frac{3m_h^2 m_{\tilde{h}}^2}{8\pi^2 v^4}\right), \tag{66}$$

where we took the unitarity bound on $\hat{\lambda}$ that follows from the four-point amplitude for δh and $\delta\Phi$ (see, e.g., [22]). This result, being proportional to the extra state mass, yields a naive cutoff $R = \frac{4\pi}{\Lambda^2}$ with inverse dependence on the new physics scale:

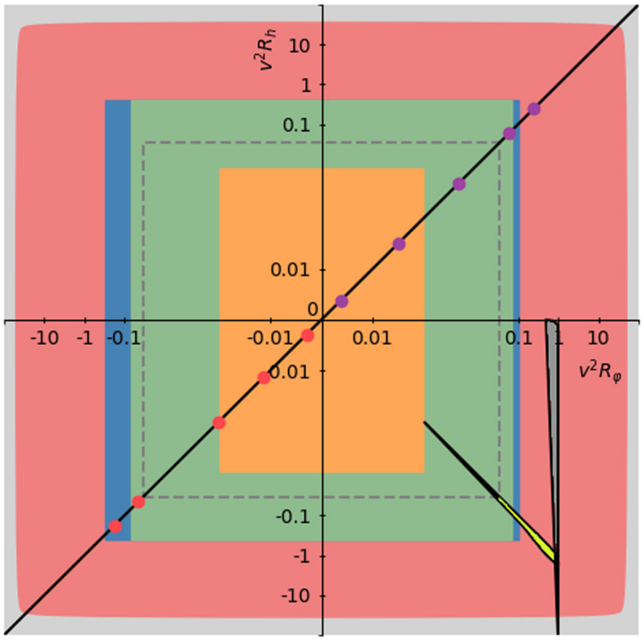

FIG. 4. Range of curvature for SMEFT and quotient theories, on the same background as Fig. 2. Two quotient theories are plotted: the yellow region shows curvature for the symmetric representation with $\langle\Phi\rangle \neq 0$, and the dark-gray region shows a hyperbolic manifold (see Sec. V). The black line shows SMEFT curvature, on which the purple and red dots represent the singlet and the symmetric representation with $\langle\Phi\rangle = 0$ examples from Sec. IV, respectively. The outermost to innermost dots are evaluated with coupling $g_* = 1$ and heavy singlet mass: 500 GeV, 1 TeV, 1.5 TeV, 2 TeV, and 4 TeV.

$$\frac{\Lambda^2}{v^2} \sim \frac{(4\pi)^3}{\lambda_{\rm SM}} \frac{v^2}{m_{\tilde{h}}^2}, \tag{67}$$

so that the largest cutoff, or the closest to the SM couplings one can get, is attained for the lowest new physics scale. How low this scale can be while still being able to assume an EFT applies can be estimated from the amplitude for W scattering, mediated by the singlets in the full theory

$$-\mathcal{A} = \frac{s}{v^2}\left(1 - c_\beta^2 \frac{s}{s - m_h^2} - s_\beta^2 \frac{s}{s - m_{\tilde{h}}^2}\right) + (s \to t). \tag{68}$$

The plot in Fig. 4 shows the region in the curvature plane of the models discussed in this section cover. In particular, for the minimum mass of the extra singlet we take the limit of $m_{\tilde{h}} \gtrsim 350$ GeV from [23] as a reference.

V. MANIFOLDS

The above HEFT cases fall into the category of manifolds with a singularity, as one can see by integrating out heavy states [7]. In contrast, one can also have that no $O(4)$-symmetric point is present and the manifold is smooth at every point. This section visualizes both types of manifolds, together with those that admit a SMEFT description. Consider (higher dimensional) cylindrical coordinates, where the gauge symmetry acts rotating along the axis, and orthogonal to this rotation we have a cylindrical radial coordinate ρ and a "height" z. Our manifolds are hypersurfaces within this five-dimensional (5D) space parametrized by h and φ^a,

$$(\rho(h)u(\varphi), z(h)), \tag{69}$$

with a line element

$$d\ell^2 = \left(\left(\frac{d\rho}{dh}\right)^2 \pm \left(\frac{dz}{dh}\right)^2\right) dh^2 + \rho(h)^2 du^2, \tag{70}$$

which defines the 4D metric, where the plus sign is for Euclidean 5D space and the minus for the metric with a $(-1, 1, 1, 1, 1)$ signature. In our basis, Eq. (14), dh^2 has a unit coefficient that can always be attained by a field redefinition. In terms of geometry, the singlet Higgs field h equals the distance in field space for fixed u. From the equation above and our basis it also follows that $F(h) = \rho(h)/v$ with $F(0) = 1$ giving $\rho(0) = v$. For convenience let us define $\theta = (h + h_0)/f$ with f a new physics scale.

The most symmetric manifolds are S^4, R^4, and $\mathcal{H}^4$, which are parametrized in our basis as

$$S^4 \quad (f\sin(\theta)u, f\cos(\theta)), \tag{71}$$

$$R^4 \quad ((h + v)u, 0), \tag{72}$$

$$\mathcal{H}^4 \quad (f\sinh(\theta)u, f\cosh(\theta)), \tag{73}$$

and yield constant (field-independent) curvature:

$$S^4, \mathcal{H}^4 \quad \begin{array}{cc} R_\varphi, & R_h \\ \pm\frac{1}{f^2}, & \pm\frac{1}{f^2} \end{array} \tag{74}$$

while the $f \to \infty$ limit yields R^4 which corresponds to the SM. Indeed, these manifolds can be described in SMEFT and correspond to composite Higgs models [24] or negative curvature models [25].

A. Quotient space theories with a singularity

A one-parameter deformation of the manifolds above takes us into quotient space with a singularity at the origin:

$$\text{deformed } S^4 \quad \left(f s_{\gamma\theta} u, \int dh \sqrt{1 - \gamma^2 c_{\gamma\theta}^2}\right), \tag{75}$$

$$\text{deformed } \mathcal{H}^4 \quad \left(f sh_{\gamma\theta} u, \int dh \sqrt{\gamma^2 ch_{\gamma\theta}^2 - 1}\right), \tag{76}$$

where $s_{\gamma\theta} = \sin(\gamma\theta)$ and the singularity is made evident by the curvature

$$\begin{array}{lll} & R_\varphi & R_h \\ \text{deformed } S^4 & \frac{1-\gamma^2}{f^2 s^2_{\gamma\theta}} + \frac{\gamma^2}{f^2}, & \frac{\gamma^2}{f^2}, \end{array} \tag{77}$$

$$\text{deformed } \mathcal{H}^4 \quad \frac{1-\gamma^2}{f^2 sh^2_{\gamma\theta}} - \frac{\gamma^2}{f^2}, \qquad -\frac{\gamma^2}{f^2}, \tag{78}$$

since the origin and would-be-$O(4)$ invariant point, $\theta = 0$, return, which seemingly presents a way to approximate the SM by sending first $f \to \infty$ while keeping $f s_{\gamma\theta_0} (f sh_{\gamma\theta_0}) = v$ constant, and then $\gamma \to 1$. Indeed, in this limit, $\partial^n R \propto (1-\gamma^2)$ and contributions to amplitudes of an arbitrary number of particles cancel. Nonetheless and quite relevantly in this limit, the singularity is just a field distance v/γ from the vacuum $h = 0$. The model in Sec. IV B with a symmetric representation taking a VEV also belongs to the quotient theories with singularities, yet it showed that the SM point cannot be reached. So it could be that the deformed manifolds have no UV completion, yet from low energy we see no indication for it. This highlights the need for a bound based purely in the EFT perspective to comprise all possibilities.

B. Smooth quotient theories

On the other hand, one could have smooth manifolds in quotient space, $\rho \neq 0 \;\; \forall \;\; h$; we take here as examples a torus and a hyperbola (in Euclidean space)

$$\text{torus} \quad ((\rho_0 + f c_\theta) u, f s_\theta), \tag{79}$$

$$\text{hyperbola} \quad ((\rho_0 + f ch_{\hat\theta}) u, f sh_{\hat\theta}), \tag{80}$$

where $\hat\theta = (\hat h(h) + \hat h_0)/f$ with $(dh/d\hat h)^2 = sh^2_{\hat\theta} + ch^2_{\hat\theta}$ as follows from our normalization in Euclidean 5D. In terms of curvature, these manifolds give

$$\begin{array}{lll} & R_\varphi & R_h \\ \text{Torus} & \frac{\cos(\theta)^2}{v^2}, & \frac{\cos(\theta)}{fv}, \end{array} \tag{81}$$

$$\text{Hyperbola} \quad \frac{ch^2_{\hat\theta}}{(ch^2_{\hat\theta} + sh^2_{\hat\theta}) v^2}, \qquad \frac{-ch_{\hat\theta}}{(ch^2_{\hat\theta} + sh^2_{\hat\theta})^2 f v}. \tag{82}$$

We see that the hyperbola does not go through the zero curvature point for any value of f, θ, always keeping a distance as the explicit model in Sec. IV B did. The torus, however, for $\theta = \pi/2$ does have both curvatures vanish, yet by construction the manifold is not R^4. Visually, for this point we are sitting atop of the torus, and for its first two derivatives it does resemble a plane; but its third derivative is nonvanishing, and indeed $R'_h = 1/f^2 v$ which is bounded from below given $\rho_0 > f$ and for $\theta = \pi/2$, $v = \rho_0$.

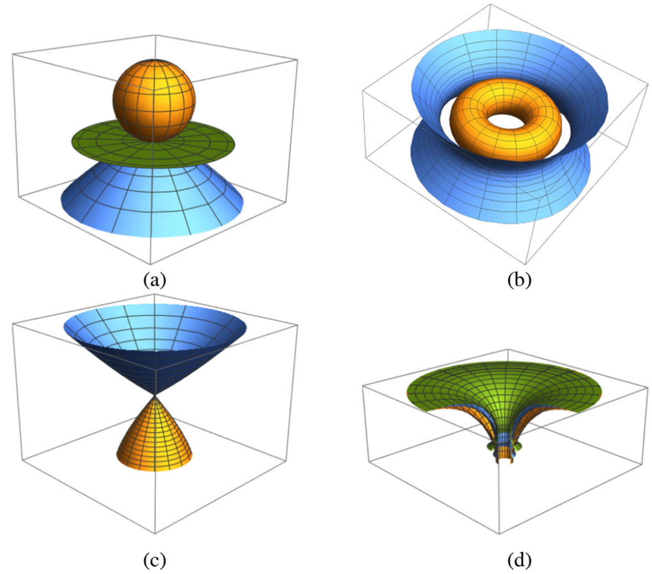

FIG. 5. Examples of manifolds which belong (a) in SMEFT or (b), (c), (d) in quotient space with the gauge symmetry action being rotation around the z axis. SMEFT manifolds in (a) correspond as follows: Composite models (yellow), the SM (green), and negative curvature models (blue). Quotient manifolds (b), (d) are smooth, while (c) presents a singularity, and both (c), (d) are in a class that resembles the SM around the vacuum. For (d), part of the manifolds has been cut out for better visualization.

This nonetheless illustrates the possibility of manifolds that do look locally like the SM to the nth derivative, yet do not go through the origin. Let us take on such a set of manifolds labeled by n

$$F_{(n)}(h) = 1 + \frac{h}{v} + c_n \left(\frac{h}{v}\right)^n, \qquad |c_n| > \frac{(n-1)^{n-1}}{n^n}. \tag{83}$$

The manifolds associated with these F_n for $n = 3, 4, 5$ are plotted in Fig. 5, and they resemble a plane and hence the SM ever more accurately for increasing n around $h = 0$.

It should be underlined that we do not know an UV completion that would yield this type of EFT, as opposed to quotient theories with singularities.

VI. OBSTACLES IN THE ROAD TO THE SM

We have encountered HEFT/SMEFT quotient theories that come from either smooth manifolds with no $O(4)$-invariant point or manifolds that get arbitrarily close to the would-be $O(4)$-invariant point, but the point itself is singular.

A number of UV complete theories yield quotient theories with singularities at the origin. From working out an explicit example, we have seen that these can only get within a finite distance of the SM point. This explicit computation relied on knowledge of the full theory, but here we attempt to give an argument as to why quotient theories are not a road to the SM model in purely low energy grounds.

Let us turn to semiclassical arguments. Consider the Higgs field as sourced by a probe particle i localized in a region σ_x and with a mass $m_i > m_h$. This configuration is, of course, short lived, yet for times smaller than the decay rates one might consider such a system. The renormalizable linear realization gives an equation of motion[4]

$$(-\Box - m_h^2)h(x) = \frac{m_i}{v}J_i(x), \tag{84}$$

where

$$\text{Spin}1/2 \quad J_i = \langle i|\bar{\psi}\psi|i\rangle, \tag{85}$$

$$\text{Spin } 1 \quad J_i = -\langle i|m_i V_\mu V^\mu|i\rangle, \tag{86}$$

and the particle state is

$$|i\rangle = \int \frac{d^3p}{(2\pi)^3}\Psi(p)\frac{a^\dagger_{i,p}}{\sqrt{2E_p}}|0\rangle. \tag{87}$$

Away from the localized source the field is

$$h(r > \sigma_x) = \frac{m_i}{v}\int \frac{d^4x d^4q}{(2\pi)^4}\frac{e^{iq(x-y)}\hat{J}_i(\vec{x})}{q^2 - m^2} \tag{88}$$

$$\simeq -\frac{m_i}{v}\frac{e^{-m_h r}}{4\pi r}, \tag{89}$$

where in the second line we assumed that the current J_i is the same as the probability density, as we shall see justified in the nonrelativistic limit.

Consider now the candidate quotient theories that resemble the Standard Model to a high degree, where examples given in the previous section are the functions $F_{(n)}$ as given in (83) or the deformed S^4, $\mathcal{H}^4$ theories (77) and (78). The solution above should be a good first approximation certainly for large distances $r > 1/m_h$ where the field value is exponentially close to the vacuum value. However, at shorter distances if our candidate theories truly present a limit in which the SM couplings are recovered, the solution should still be a good approximation. The field value nonetheless increases with decreasing distance, and if there is a singularity in this SM limit, it is just a distance $v/\gamma \simeq v$ away in field space. Conversely, for smooth quotient theories, even if our series example $F_{(n)}$ resembles the SM locally around the vacuum, the corrections in Eq. (84) read $1 + nc_n(h/v)^n$ with $nc_n \sim 1$ for $n \gg 1$ and would dominate over the SM for $h \sim v$. This is indeed the same condition for both types of theories and yields a naive minimum distance or cutoff

$$\frac{h(\sigma_x < r < m_h^{-1})}{v} \simeq \frac{m_i}{v}\frac{1}{4\pi v r}, \tag{90}$$

$$\frac{h(r_0)}{v} \sim 1 \quad \text{for } \frac{1}{r_0} \equiv \Lambda \sim 4\pi v\frac{v}{m_i}. \tag{91}$$

This points at a cutoff an inverse coupling factor higher than other estimates based on perturbative unitarity. Nevertheless, quantum mechanics has something to say about our implicit assumption $\sigma_x < r_0$. Indeed, $r_0 \sim (m_i^2/4\pi v^2)m_i^{-1}$ is smaller than the inverse mass of a particle for perturbative couplings (which is the case for the SM), but in order to localize the particle in a distance smaller than the inverse mass, the uncertainty principle dictates a range of momenta that extends to the relativistic regime. In this high energy limit, our current J_i suffers a relativist factor m/E suppression as an explicit evaluation of the matrix elements shows when going beyond the nonrelativistic approximation. For a fermion, one has

$$J_i(x) = \int \frac{d^3p d^3k}{(2\pi)^6}\frac{\bar{u}(k)u(p)}{\sqrt{2E_p 2E_k}}e^{i(p-k)x}\Psi^*(k)\Psi(p), \tag{92}$$

which implies that the space integral over the source J_i is suppressed and the field value at a distance $r > \sigma_x$ is

$$\frac{h(\sigma_x < r)}{v} = \frac{N(m_i\sigma_x)}{4\pi v r}\frac{m_i}{v^2} = \frac{N(\sigma_x m_i)}{r m_i}\alpha_i, \tag{93}$$

$$N(m_i, \sigma_x) = \frac{\int d^3k (m_i/E_p)|\Psi(p)|^2}{\int d^3k|\Psi(p)|^2}, \qquad \alpha_i = \frac{m_i^2}{4\pi v^2}, \tag{94}$$

which is the same result for spins $1/2$ and 1. This suppression implies that the prefactor of α_i in Eq. (93) is at most order one, which would then require an order one α_i to probe $(h/v) \sim 1$. Note that this α_i will be at the edge of perturbative unitarity, although loop corrections will be suppressed by $\sim 1/(4\pi)$.

As an estimate, we take a Gaussian distribution $\Psi \sim e^{-(p\sigma_x)^2/2}$ and evaluate the potential at a distance $r = 2\sigma_x$ which encloses 95% of the probability density to find that with $\alpha_i \sim 2$ the cutoff, or inverse distance, where we would probe $h \sim v$ would be $r_0 = 0.6 m_i^{-1}$,

$$\Lambda \sim \sqrt{\frac{8\pi\sigma_x m_i}{N(\sigma_x m_i)}}\bigg|_{m_i\sigma\sim 0.3} v \simeq 2 \text{ TeV}. \tag{95}$$

The nature of EWSB and the question of whether a symmetric $O(4)$ point exits should be independent of the introduction of our probe particle i, although admittedly the fact that one would require couplings on the perturbative edge makes the above a rough estimate.

The naive scaling from Eq. (90) does, however, point toward the typical scale for nonperturbative effects. This is

[4]The spin 0, 1 case has an extra h/v times the source which we dropped.

indeed the natural scale for answering nonlocal questions about our theory. While the detailed study of this effect will be presented elsewhere [26], here we sketch the modifications in a well-known nonperturbative effect, sphalerons, whose energy is

$$E_{\mathrm{sph}} \sim \frac{4\pi v}{g}. \tag{96}$$

In particular, the topological argument by Manton [27] has to do with a loop (parametrized by μ) of mappings from the sphere at spatial infinity to the vacuum manifold, characterized by our unit vector u, i.e., $u(\theta,\phi;\mu)$, and holds regardless of the Higgs singlet role. Nonetheless, the boundary conditions *to find the energy* of the potential barrier have to be drastically changed in quotient theories. Indeed, the proposed field at the top of the barrier $\mu=\pi/2$ in [27] is ($\mathbf{h}=h(r)u$),

$$\mathbf{h}=h(r)\begin{pmatrix} s_\mu s_\theta c_\phi \\ s_\mu s_\theta s_\phi \\ s_\mu c_\mu (c_\theta - 1) \\ s_\mu^2 c_\theta + c_\mu^2 \end{pmatrix}, \qquad \mathrm{B.C.}\begin{cases} h(0)=0, \\ h(\infty)=v. \end{cases} \tag{97}$$

In particular, the condition at the origin, where the Higgs field goes to its symmetry preserving $O(4)$ symmetric point, is demanded to remove dependence on angular variables of the Higgs doublet at the origin where θ,ϕ are ill-defined. For quotient theories, it is clear that this does not apply given that an $O(4)$ point is absent or singular. One can introduce a radial dependent function on u itself such that

$$u(\theta,\phi,r\to\infty)=u_\infty, \qquad u(\theta,\phi,r\to 0)\to u_0. \tag{98}$$

The boundary conditions on h would naively be $h'(0)=0$. In either case, the quotient theory effect is an order one modification that serves as a handle to tell quotient theories apart from the Standard Model.

VII. SUMMARY

This work studied the quotient space HEFT/SMEFT and the potential limits to recover the SM other than via SMEFT with the use of a geometric formulation. Explicit examples, which include perturbative UV complete models, can and will be told apart from the SMEFT case by future experiments via the projection of measurements on the curvature plane defined from the WW scattering and $WW\to hh$ amplitudes (see Fig. 4). These examples of quotient space HEFT/SMEFT theories do not offer a limit to recover the SM and possess a finite cutoff. In contrast to these, quotient theories were formulated in Sec. V that resemble the SM amplitudes for arbitrary precision and number of particles. While these theories look like the SM model around the vacuum, at a Higgs-singlet distance of $\sim v$ they reveal their quotient space nature. Making use of semiclassical arguments to displace the Higgs field by $\sim v$, we find an argument for general theories in quotient space to be distinguishable from the SM when probing the theory at an energy (inverse distance) of at most $4\pi v/g_{\mathrm{SM}}$. Our discussion applies to quotient theories both with and without singularities (nonanalyticities). The most pressing outstanding question is the characterization of experimental signatures that follow from the semiclassical arguments given here.

ACKNOWLEDGMENTS

R. A. and M. W. are supported by the STFC under Grant No. ST/T001011/1.

[1] I. Brivio and M. Trott, The standard model as an effective field theory, Phys. Rep. **793**, 1 (2019).
[2] T. Appelquist and J. Carazzone, Infrared singularities and massive fields, Phys. Rev. D **11**, 2856 (1975).
[3] F. Feruglio, The chiral approach to the electroweak interactions, Int. J. Mod. Phys. A **08**, 4937 (1993).
[4] B. Grinstein and M. Trott, A Higgs-Higgs bound state due to new physics at a TeV, Phys. Rev. D **76**, 073002 (2007).
[5] R. Alonso, E. E. Jenkins, and A. V. Manohar, A geometric formulation of Higgs effective field theory: Measuring the curvature of scalar field space, Phys. Lett. B **754**, 335 (2016).
[6] R. Alonso, E. E. Jenkins, and A. V. Manohar, Geometry of the scalar sector, J. High Energy Phys. 08 (2016) 101.
[7] T. Cohen, N. Craig, X. Lu, and D. Sutherland, Is SMEFT enough?, J. High Energy Phys. 03 (2021) 237.
[8] A. Helset, A. Martin, and M. Trott, The geometric standard model effective field theory, J. High Energy Phys. 03 (2020) 163.
[9] T. Cohen, N. Craig, X. Lu, and D. Sutherland, Unitarity violation and the geometry of Higgs EFTs, J. High Energy Phys. 12 (2021) 003.
[10] A. Falkowski and R. Rattazzi, Which EFT, J. High Energy Phys. 10 (2019) 255.
[11] A. Falkowski, S. Rychkov, and A. Urbano, What if the Higgs couplings to W and Z bosons are larger than in the Standard Model?, J. High Energy Phys. 04 (2012) 073.
[12] S. Coleman, J. Wess, and B. Zumino, Structure of phenomenological lagrangians. I, Phys. Rev. **177**, 2239 (1969).
[13] A. Hatzinikitas, A note on Riemann normal coordinates, arXiv:hep-th/0001078.

[14] C. Hays, A. Helset, A. Martin, and M. Trott, Exact SMEFT formulation and expansion to $\mathcal{O}(v^4/\Lambda^4)$, J. High Energy Phys. 11 (2020) 087.

[15] G. Aad *et al.* (ATLAS Collaboration), Combined measurements of Higgs boson production and decay using up to 80 fb^{-1} of proton-proton collision data at $\sqrt{s} = 13$ TeV collected with the ATLAS experiment, Phys. Rev. D **101**, 012002 (2020).

[16] A. Tumasyan *et al.* (CMS Collaboration), Search for Higgs boson pair production via vector boson fusion with highly Lorentz-boosted Higgs bosons in the four b quark final state at $\sqrt{s} = 13$ TeV (2021), http://cds.cern.ch/record/2776802.

[17] M. Cepeda *et al.*, Report from working group 2: Higgs physics at the HL-LHC and HE-LHC, CERN Yellow Rep. Monogr. **7**, 221 (2019).

[18] A. Abada *et al.* (FCC Collaboration), FCC-ee: The Lepton Collider: Future circular collider conceptual design report volume 2, Eur. Phys. J. Special Topics **228**, 261 (2019).

[19] F. Bishara, R. Contino, and J. Rojo, Higgs pair production in vector-boson fusion at the LHC and beyond, Eur. Phys. J. C **77**, 481 (2017).

[20] I. Brivio, T. Corbett, O. J. P. Éboli, M. B. Gavela, J. Gonzalez-Fraile, M. C. Gonzalez-Garcia, L. Merlo, and S. Rigolin, Disentangling a dynamical Higgs, J. High Energy Phys. 03 (2014) 024.

[21] A. Adams, N. Arkani-Hamed, S. Dubovsky, A. Nicolis, and R. Rattazzi, Causality, analyticity and an IR obstruction to UV completion, J. High Energy Phys. 10 (2006) 014.

[22] B. W. Lee, C. Quigg, and H. B. Thacker, Weak interactions at very high-energies: The role of the Higgs boson mass, Phys. Rev. D **16**, 1519 (1977).

[23] M. Aaboud *et al.* (ATLAS Collaboration), Search for heavy resonances decaying into WW in the $e\nu\mu\nu$ final state in pp collisions at $\sqrt{s} = 13$ TeV with the ATLAS detector, Eur. Phys. J. C **78**, 24 (2018).

[24] G. Panico and A. Wulzer, The composite Nambu-Goldstone Higgs, Lect. Notes Phys. **913**, 1 (2016).

[25] R. Alonso, E. E. Jenkins, and A. V. Manohar, Sigma models with negative curvature, Phys. Lett. B **756**, 358 (2016).

[26] R. Alonso and M. West (to be published).

[27] N. S. Manton, Topology in the Weinberg-Salam theory, Phys. Rev. D **28**, 2019 (1983).